Role of the C-terminal extension stacked on the re-face of the isoalloxazine ring moiety of the flavin adenine dinucleotide prosthetic group in ferredoxin-NADP+ oxidoreductase from Bacillus subtilis

Role of the C-terminal extension stacked on the *re*-face of the isoalloxazine ring moiety of the flavin adenine dinucleotide prosthetic group in ferredoxin-NADP+ oxidoreductase from *Bacillus subtilis*

Daisuke Seo[1]*, Tomoya Asano[2], Hirofumi Komori[3], Takeshi Sakurai[1]

[1]Division of Material Science, Graduate School of Natural Science and Technology, Kanazawa University, Kakuma, Kanazawa, Ishikawa 920-1192, Japan

[2]Division of Functional Genomics, Advanced Science Research Center, Kanazawa University, Takaramachi 13-1, Kanazawa, Ishikawa 920-0934, Japan

[3]Faculty of Education, Kagawa University, 1-1 Saiwai, Takamatsu, Kagawa 760-8522, Japan

*To whom corresponding: Daisuke Seo

Division of Material Science, Graduate School of Natural Science and Technology, Kanazawa University, Kakuma, Kanazawa, Ishikawa 920-1192, Japan, Tel: +81-76-264-5683, Fax: +81-76-264-5742, E-mail: dseo@se.kanazawa-u.ac.jp

Abbreviations:

Ad; adrenodoxin, AdR; adrenodoxin reductase, FAD; flavin adenine dinucleotide, Fd; ferredoxin, FNR; ferredoxin-NAD(P)+ oxidoreductase, G6P; glucose-6-phosphate, G6PDH; glucose-6-phosphate dehydrogenase, GR; glutathione reductase, HEPES; 4-(2-hydroxyethyl)-1-piperazineethanesulfonic acid, K_d; dissociation constant, K_m; Michaelis constant, MALDI TOFMS; Matrix Assisted Laser Desorption/Ionization Time of Flight Mass Spectrometry, Pd; putidaredoxin, PdR; putidaredoxin reductase, SDS-PAGE; sodium dodecyl sulfate-polyacrylamide gel electrophoresis, Td; thioredoxin, TrxR; bacterial NADPH-thioredoxin reductase, Tris; tris(hydroxymethyl)aminomethane, WT; wild type.

Abstract

Ferredoxin-NADP$^+$ oxidoreductase [EC 1.18.1.2] from *Bacillus subtilis* (*Bs*FNR) is homologous to the bacterial NADPH-thioredoxin reductase, but possesses a unique C-terminal extension that covers the *re*-face of the isoalloxazine ring moiety of the flavin adenine dinucleotide (FAD) prosthetic group. In this report, we utilize *Bs*FNR mutants depleted of their C-terminal residues to examine the importance of the C-terminal extension in reactions with NADPH and ferredoxin (Fd) from *B. subtilis* by spectroscopic and steady-state reaction analyses. The depletions of residues Y313 to K332 (whole C-terminal extension region) and S325 to K332 (His324 intact) resulted in significant increases in the catalytic efficiency with NADPH in diaphorase assay with ferricyanide, whereas K_m values for ferricyanide were increased. In the cytochrome *c* reduction assay in the presence of *B. subtilis* ferredoxin, the S325-K332 depleted mutant displayed a significant decrease in the turnover rate with an Fd concentration range of 1 to 10 μM. The Y313-K332 depleted mutant demonstrated an increase in the rate of the direct reduction of horse heart cytochrome *c* in the absence of Fd. These data indicated that depletion of the C-terminal extension plays an important role in the reaction of *Bs*FNR with ferredoxin.

1. Introduction

Ferredoxin-NAD(P)$^+$ oxidoreductase ([EC 1.18.1.2], [EC 1.18.1.3], FNR) is a member of the dehydrogenase family of the flavoprotein superfamily (Aliverti et al., 2008; Dym and Eisenberg, 2001; Correll et al., 1993). FNR catalyzes the redox reaction between the two electron carrier nucleotides, NAD(P)H, and the one electron carrier iron-sulfur proteins, ferredoxin (Fd), adrenodoxin (Ad) and putidaredoxin (Pd), and also the low molecular weight flavoprotein, flavodoxin. In photosynthesis, FNR catalyzes the reduction of NADP$^+$ to NADPH by photochemically reduced Fd (Sétif, 2001; Knaff and Hirasawa, 1991). In non-photosynthetic processes, FNR and its isoforms catalyze the reduction of Fd, Ad and Pd with NAD(P)H. In the latter case, reduced iron-sulfur proteins play an indispensable role as a low redox potential electron donor in a variety of metabolic processes including cytochrome P450-dependent hydroxylation, nitrogen fixation and the tolerance of active oxygen species. (Aliverti et al., 2008; Knaff and Hirasawa, 1991; Bianchi et al., 1993; Munro et al., 2007; Ewen et al., 2011).

FNRs generally consist of two nucleotide-binding domains that are typically found among the FAD-dependent dehydrogenase family (Aliverti et al., 2008; Dym and Eisenberg, 2001; Correll et al., 1993). Phylogenic and structural information on FNR and its isoforms indicates that FNRs are categorized into five groups (Aliverti et al., 2008; Ceccarelli et al., 2004; Seo et al., 2004; Muraki et al., 2010). FNRs from green sulfur bacteria, Firmicutes and thermophiles (designated as TrxR-type FNRs) exhibit significant conservation of structural topology with bacterial NADPH-thioredoxin reductase (TrxR) (Seo et al., 2004; Muraki et al., 2010; Komori et al., 2010), whereas adrenodoxin reductase (AdR) and putidaredoxin reductase (PdR) exhibit conservation of structural topology with glutathione reductase (GR) (Aliverti et al., 2008; Dym and Eisenberg, 2001). The structural topologies of these FNR groups are distinct from those of FNRs from plastid, cyanobacteria and proteobacteria. The latter FNRs are structurally related to phthalate dioxygenase reductase, NADPH-cytochrome P450 reductase and cytochrome *b*5 reductase (Aliverti et al., 2008; Dym and Eisenberg, 2001; Correll et al., 1993; Karplus and Faber, 2004). Despite the differences in structural topology, similar arrangements of amino acid residues are often found around the isoalloxazine ring moiety of the FAD prosthetic group among FNR and its relatives. One such arrangement of amino acid residues involves the aromatic residues stacked on the isoalloxazine ring moiety of the FAD prosthetic group. The functional role of these residues has been extensively studied in plastid-type FNRs. Mutational analyses of FNRs from cyanobacteria (Piubelli et al., 2000; Nogués et al., 2004; Tejero et al., 2005) and Apicomplexa (Baroni et al., 2011), and cytochrome P450 BM3 (Neeli et al., 2005) display altered selectivity

3

towards NADH/NADPH upon replacement of the aromatic residues on the *re*-face of the ring. In the case of TrxR-type FNRs from *Chlorobaculum tepidum* (*Ct*FNR) and *Bacillus subtilis* (*Bs*FNR), replacement of the *re*-face Phe and His, respectively, did not significantly affect its selectivity and reactivity to NAD(P)H (Muraki et al., 2010; Komori et al., 2010).

The crystal structures of *Ct*FNR (Muraki et al., 2010), *Thermus thermophilus* HB8 (PDB code: 2ZBW) (Mandai et al., 2009a) and *Bs*FNR (Komori et al., 2010) have revealed that these FNRs possess homologous structural topology with the TrxR, but only the TrxR-type FNRs possess the two conserved aromatic residues on the *si*- and *re*-face of the ring (Fig. 1). In the case of *Bs*FNR, Tyr50 on the *si*-face and His324 on the *re*-face of the isoalloxazine ring moiety of the FAD prosthetic group stacked almost in parallel to the isoalloxazine ring moiety of the FAD prosthetic group at a distance of approximately 3.5 Å (Komori et al., 2010). The five amino acid residues following His324 form a unique short α-helix in the crystal structure of *Bs*FNR and cover the *re*-face of the ring (Figure 1). A structurally related TrxR from *Escherichia coli* (*Ec*TrxR) lacks the corresponding aromatic residues and C-terminal short α-helix (Waksman et al., 1994). The role of the C-terminal extension in *Bs*FNR including the *re*-face His324 residue remains unclear. The crystal structure of *Bs*FNR in the $NADP^+$-bound form indicates that *Bs*FNR and *Ec*TrxR share similarities in their $NADP^+$ binding mode (Komori et al., 2010) and accordingly, a drastic domain motion would be required for hydride ion transfer between $NAD(P)^+$/H and the FAD prosthetic group as previously proposed for *Ec*TrxR (Lennon et al., 2000). In such a scenario, the C-terminal extension would prevent the nicotinamide ring moiety of $NADP^+$/H from coming into close contact with the isoalloxazine ring moiety in TrxR-type FNR, thereby participating in the reaction with NAD(P)H. To analyze the functional role of the C-terminal extension of *Bs*FNR during interactions with Fd and NAD(P)H, we performed a reaction analysis of *Bs*FNR mutants with specific alterations designed to impair the C-terminal region.

2. Results

2.1 Preparation of WT and mutant FNRs

Two C-terminal depleted *Bs*FNR mutants *Δ*Y313-K332 and *Δ*S325-K332 (hereafter designated as *Δ*Y313 and *Δ*S325, respectively) were purified to homogeneity using a method for the preparation of recombinant wild type (WT) enzyme (Fig. S1). The molecular mass of the WT *Bs*FNR polypeptide migrated with an apparent molecular mass of 40 kDa on a sodium dodecyl sulfate-polyacryl amide gel electrophoresis (SDS-PAGE) gel. *Δ*S325 *Bs*FNR also migrated with an apparent molecular mass similar to that of WT and the *Δ*Y313 mutant had an apparent molecular mass of approximately 38 kDa on an SDS-PAGE gel. Matrix Assisted Laser Desorption/Ionization Time of Flight Mass Spectrometry (MALDI-TOFMS) analysis of the WT *Bs*FNR in native form displayed major peaks with masses of 36749 Da and 37523 Da. The corresponding values calculated from the DNA sequence with or without FAD were 37625 and 36839 Da, respectively. Similarly, mutant protein peak sizes of 34431 Da and 35179 Da (34496 and 35281 Da by sequence) for *Δ*Y313 and 35866 Da and 36624 Da (35932 and 36718 Da by sequence) for *Δ*S325 mutants correlated with WT peak sizes (Fig. S2). All of the purified FNRs eluted as a single peak during gel-permeation chromatography. The deduced apparent molecular mass of WT *Bs*FNR was approximately 97 kDa (Table 1). ΔY313 and ΔS325 mutants also exhibited a single peak with a deduced apparent molecular mass of approximately 94 kDa. These data confirm that all FNRs utilized in this report were present as homo-dimers in solution.

2.2 Spectroscopic properties

The UV-visible absorption spectra of the *Δ*Y313 and *Δ*S325 mutants exhibited a slight blue-shift of the FAD transition band in the near-UV region with peaks at approximately 380 nm when compared to that of WT (Fig. 2A). These blue shifts are likely due to changes in the environment of the FAD prosthetic group including a loss of hydrogen bonding with the Ser325 and Thr326 residues, a decrease in the polarity of the environment and/or a loss of the dipole field of the C-terminal helix (Yagi et al., 1980; Heelis. 1982). Absorption coefficients of WT and mutated *Bs*FNRs at the λ_{max} of approximately 460 nm exhibited similar values (12.3 - 12.6 $mM^{-1}cm^{-1}$, Table 1).

Addition of $NADP^+$ to the FNR solution induced a shift in the flavin bands which produced troughs at approximately 450 and 480 nm, and peaks at approximately 470 and 505 nm on the difference spectra (Fig. 2B). The Δabsorbance of the difference

spectra at 505-6 nm minus 480-1 nm for $\mathit{\Delta}$Y313 and $\mathit{\Delta}$S325 mutants increased when compared to that of WT BsFNR for the blue

shift of the absorption bands in the NADP$^+$-free oxidized form and exhibited a similar shape after addition of NADP$^+$. The plots

of the absorption changes (ΔA_{505-6} minus ΔA_{480-1}) on the difference spectra against the NADP$^+$ concentration provided saturation

curves (Fig. 2C). Dissociation constant (K_d) values of the mutated BsFNRs significantly decreased to less than half that of WT

BsFNR (Table 1), indicating an increase in the stability of the NADP$^+$-FNR complex upon deletion of the C-terminal extension.

2.3 Steady-state reactions with NADPH and ferredoxin

To evaluate the reactivity of WT and mutated BsFNRs with NADPH, a diaphorase assay was performed using potassium

ferricyanide as an electron acceptor (Table 1). Upon depletion of the C-terminal extension, the K_m value for ferricyanide

drastically increased (Table 1). Although the k_{cat} values for WT and mutated FNRs at 1 mM NADPH were similar, the K_m values

for NADPH of the C-terminal depletion mutants significantly decreased when compared to WT (Table 1). Together with the

obtained K_d values for NADP$^+$, depletion of the C-terminal extension resulted an increase in the reactivity with NADP$^+$/H.

For the assay of FNR under steady-state reaction conditions, the Fd reduction rate is often evaluated by the cytochrome c

reduction assay utilizing cytochrome c as a final electron acceptor. Under the assay conditions outlined in this report,

concentrations of the acceptor proteins were much larger than that of the donor proteins (FNR (-10 nM) < Fd (1-10 μM) <

cytochrome c (0.1 mM)). This design minimized the effects of side reactions on the estimation of the Fd-dependent cytochrome c

reduction rate except for direct cytochrome c reduction by FNR. WT and $\mathit{\Delta}$S325 BsFNR exhibited relatively low direct

cytochrome c reduction rates in an NADPH concentration range of 1-200 μM (< 1.5 s^{-1} and < 3.5 s^{-1}, respectively). However, the

$\mathit{\Delta}$Y313 mutant displayed an enhanced direct cytochrome c reduction rate which was approximately $15 - 20$ s^{-1} at an NADPH

concentration range of 1-200 μM at 0.1 mM cytochrome c. An addition of BsFd did not substantially increase the rate of

cytochrome c reduction. Accordingly, we could not estimate the rate of Fd-dependent cytochrome c reduction for the $\mathit{\Delta}$Y313

mutant. The rates for the $\mathit{\Delta}$S325 mutant decreased to less than half that of WT BsFNR at 5 μM NADPH (Fig. 3). The linear

dependency of the reduction rate for the $\mathit{\Delta}$S325 mutant on the BsFd concentration might indicate that the affinity of $\mathit{\Delta}$S325

BsFNR to BsFd was considerably reduced when compared to WT.

3. Discussion

Depletion of the C-terminal extension of *Bs*FNR slightly increased its reactivity with NADP^{+}/H, but significantly reduced its reactivity with *Bs*Fd in the steady-state assay. Because the rate for the reductive half reaction of *Bs*FNR in the diaphorase assay is more than an order of magnitude faster than that of the observed oxidative half reaction in the cytochrome *c* reduction assay, the presence of the C-terminal extension may increase the turnover rate for the physiological reaction. These results are useful in the context of the assignment of TrxR-type FNR genes and the investigation into the shared structural topology of TrxR-type FNR and TrxR. Crystal structure analyses suggested that *Bs*FNR and *Ec*TrxR bind NADP^{+}/H with a similar binding mode (Komori et al., 2010; Waksman et al., 1994; Lennon et al., 2000); however, amino acid sequence and structural information predict that *Bs*FNR uses a distinct mode to bind Fd and Fld. In *Ec*TrxR, thioredoxin (Td) reduction is catalyzed via the redox-active two cysteine residues (Cys135 and Cys138 in the *Ec*TrxR numbering scheme) present on the surface of the NADPH-binding domain and the Td-binding site is almost completely conserved in TrxR (Waksman et al., 1994; Lennon et al., 2000). In contrast, FNR catalyzes the two separate single electron transfer to the external soluble protein. Because electron transfer to and from Fd requires close contact of the Fe-S cluster with the isoalloxazine ring moiety of the FAD prosthetic group at a distance for efficient electron tunneling (Moser et al., 2010), the Fd binding sites of plastid-type FNRs in co-crystals are close to the *re*-face of the isoalloxazine ring (Kurisu et al., 2001; Medina and Gómez-Moreno, 2004). However, the binding modes of Fd have not been determined for TrxR-type FNRs. Our results suggest that the C-terminal extension is involved in Fd binding and/or an electron transfer. Fd binding around the C-terminal region was also proposed in a recent report on the *Tt*FNR-*Tt*Fd fusion protein of a TrxR type-FNR where fusion of the *Tt*Fd domain to the N-terminus of *Tt*FNR did not exhibit a reduction of cytochrome P450, whereas fusion of the *Tt*Fd domain to the C-terminus successfully reduced cytochrome P450 (Mandai et al., 2009b). TrxR-type FNRs presumably evolved to enhance their reactivity with Fd by extending the C-terminus beyond the *re*-face of the isoalloxazine ring from the original structure shared with TrxR. The open conformation observed in the *Bs*FNR crystal structure (Komori et al., 2010) enables the *Bacillus thermoproteolyticus* Fd (*Bt*Fd) (Fukuyama et al., 1989) to approach the isoalloxazine ring with a distance of approximately 9 Å between the Fe2 atom of the [4Fe-4S] cluster on *Bt*Fd and the C8M atom of FAD in *Bs*FNR without steric crush (Fig. S3). These data are within the range of distances found for many natural intermolecular electron transfer systems (Moser et al., 2010). This unique open conformation in the crystal structures of TrxR-type FNRs (Muraki et al., 2010; Komori et

7

al., 2010) is distinct from the FR and FO forms reported in crystals of *Ec*TrxR (Waksman et al., 1994; Lennon et al., 2000). In the C-terminal extension region of *Bs*FNR, a stretch of positively charged residues Lys317, Arg319 and Lys332 is present (Fig. S3), but the Lys and Arg residues in the C-terminal extension region are not highly conserved except for Arg319 (Fig. 1B). Furthermore, the C-terminal extension region varies in length and amino acid composition depending on the organism. With regard to the His324 residue, the replacement of the C-terminus Tyr residue, (the counterpart of His324 in plastid-type FNRs) decreases its reactivity with Fd (Nogués et al., 2004).

4. Materials and Methods

4.1 Preparations of WT BsFNR, mutant BsFNRs and B. subtilis Fd

WT *Bs*FNR was overexpressed in *E. coli* cells. The open reading frame of the *yumC* gene was cloned by PCR utilizing *B. subtilis subsp. subtilis str. 168* genome as a template and both Fwd (5'-ATGCGAGAGGATACAAAGGTT-3') and Rev (5'-GCAGACACAAGCTCCTTT-3') primers. The PCR product was blunted (Mighty Cloning Reagent Set (Blunt End), Takara Bio Company, Otsu, Japan) and ligated into the pETBlue-1 vector (Novagen, Merck KGaA, Darmstadt, Germany). The obtained DNA sequence of the open reading frame differed from the previously reported one (Seo et al., 2009). The open reading frame of the previously reported one contained additional 48 nucleotides encoding 16 amino acid residues, (IEFLPGRCNHSHNQYS), beyond the C-terminal Lys332 of the wild-type protein because of the insertion of a stop codon into an inappropriate position. The resulting plasmid was transformed into Tuner(DE3)pLacI cells (Novagen). Expression and purification were performed according to the methods described in (Seo et al., 2009) with the following modifications: Pre-cultivated cells were resuspended in terrific broth medium in place of Luria-Bertani medium with the same concentrations of antibiotics. After DyeMatrex Red A affinity column chromatography, buffer was exchanged by dialysis to 10 mM 4-(2-hydroxyethyl)-1-piperazineethanesulfonic acid (HEPES)-NaOH buffer (pH 7.0). Dialyzed FNR-containing solution was applied to a hydroxyapatite column (CHT Ceramic Hydroxyapatite Type I (20 μm), BioRad Lab. Inc., CA, U.S.A.) and eluted with a linear gradient of 10 mM HEPES-NaOH (pH 7.0) to 500 mM potassium phosphate (pH 7.0) buffers. Yellow fractions were further purified using Mono Q anion exchange column chromatography (Mono Q 10/100, GE healthcare, Buckinghamshire, UK) with a linear gradient of 0 – 400 mM NaCl in 20 mM tris(hydroxymethyl)aminomethane (Tris)-HCl buffer.

Expression vectors for mutated *Bs*FNRs containing deletions of the C-terminal extension region were constructed by introducing a stop codon TAA using a Quikchange protocol, the plasmid encoding the WT *Bs*FNR sequence as a template and the primers described in the Supplemental materials section (Table S1). Mutated *Bs*FNRs were expressed and purified according to a method similar to that used for the purification of WT *Bs*FNR. *B. subtilis* Fd was expressed in *E. coli* cells under the control of the *nprE* promoter and purified according to the methods similar to those described in (Seo et al., 2009).

9

4.2 Steady-state enzyme assays

The NADPH diaphorase assay using potassium ferricyanide as an electron acceptor was performed in 20 mM HEPES-NaOH buffer (pH 7.0) in the presence of 5 mM glucose-6-phosphate (G6P, Oriental Yeast Co., Ltd., Japan), 5 U ml^{-1} glucose-6-phosphate dehydrogenase (G6PDH, *Leuconostoc mesenteroides*; Biozyme Laboratories, Blaenavon, UK), 2 nM FNR together with NADPH (Oriental Yeast Co., Ltd., Tokyo, Japan) and potassium ferricyanide. Assays were performed at 25°C under aerobic conditions by monitoring the decrease in absorbance at 420 nm or 440 nm utilizing a double beam spectrophotometer (V-560, JASCO, Tokyo, Japan).

NADPH-dependent cytochrome *c* reduction in the presence or absence of Fd from *B. subtilis* (*Bs*Fd) was assayed in 20 mM HEPES-NaOH buffer (pH 7.0) containing 2-5 U ml^{-1} G6PDH, 5 mM G6P, 0.1 mM horse heart cytochrome *c* (Nacalai Tesque, Kyoto, Japan) and 2 – 10 nM FNRs together with Fd from *B. subtilis* and NADPH at 25°C. Additional NaCl from the *Bs*Fd stock solution was less than 2 mM. The amount of reduced horse heart cytochrome *c* was estimated by monitoring the absorption changes at 550 nm with a $\Delta\varepsilon$ value of 21 mM^{-1} cm^{-1}. Each data point is an average of three independent measurements. Horse heart cytochrome *c* was further purified by cation exchange chromatography (TSK Gel SP-5PW, Tosoh, Japan) and desalted via dialysis before use.

Turnover rates were calculated by subtracting the respective assay blank containing all of the assay reagents except for FNRs. K_m and k_{cat} values were evaluated by nonlinear regression analysis using the Michaelis-Menten equation on the IgorPro (ver. 5.02) software (WaveMetrics, USA). Turnover rates are expressed as the number of NADPH molecules consumed by one molecule of native-form FNR.

Protein and substrate concentrations were determined using the extinction coefficients for WT *Bs*FNR (ε_{457}= 12.3 mM^{-1} cm^{-1}, Seo et al., 2004), ΔY313 mutant (ε_{457}= 12.6 mM^{-1} cm^{-1}), ΔS325 mutant (ε_{457}= 12.3 mM^{-1} cm^{-1}), *B. subtilis* Fd (ε_{390} = 16.0 mM^{-1} cm^{-1}, Green et al., 2003), potassium ferricyanide (ε_{420} = 1.02 mM^{-1} cm^{-1}) and NADPH (ε_{340} = 6.2 mM^{-1} cm^{-1}).

4.3 Miscellaneous methods

The UV-visible absorption spectra were measured with a double beam spectrophotometer (V-560, JASCO) at room temperature. For K_d determination, 1–10 μl of NADP$^+$ stock solutions (1 – 100 mM) were added to each cuvette containing

*Bs*FNRs in 2 ml of 20 mM HEPES-NaOH buffer (pH 7.0) in a sample cell and 2 ml of 20 mM HEPES-NaOH buffer (pH 7.0) in the reference cell. Spectra were recorded after incubation for a few minutes at room temperature. Difference spectra were obtained by subtracting the control spectrum recorded prior to the addition of the substrates from the experimentally obtained spectra after correcting for the volume changes. K_d values were determined according to the method described in a previously published study (Batie and Kamin, 1984).

SDS-PAGE analysis was performed as described in (Laemmli, 1970). Protein bands on a 12 % gel were visualized with Coomassie Brilliant Blue R-250. Molecular masses of the native forms of the enzymes were deduced by gel-permeation chromatography on a Superdex-200 10/300 column (GE healthcare, USA) at a flow rate of 0.4 ml min^{-1} utilizing 20 mM Tris-HCl buffer (pH 8.0) containing 200 mM NaCl. The molecular mass standard was purchased from Sigma-Aldrich (Kit for Molecular Weights 12,000-200,000, MWGF200, USA). MALDI TOFMS analysis was performed utilizing an Ab Sciex 4800 Plus MALDI TOF/TOF^{TM} analyzer in linear mode. Sinapic acid was used as a matrix. Each data point is expressed as a mean value of the 40 times integration of 50 shots at a laser intensity of 3000. BSA was used as the molecular standard.

Absorption coefficients for WT and mutated *Bs*FNRs were determined by the heat denaturation method (Aliverti et al., 1999). Protein solutions containing approximately 10 µM FNRs in 10 mM HEPES-NaOH buffer (pH 7.0) were incubated in a boiling water bath for 10 minutes in the dark. Denatured proteins were separated by centrifugation at 15,000 g for 30 min. The FAD concentration in the supernatant was determined using the extinction coefficient of 11.3 mM^{-1}cm^{-1} at 450 nm.

References

Aliverti, A., Pandini, V., Pennati, A., de Rosa, M., Zanetti, G., 2008. Structural and functional diversity of ferredoxin-NADP$^+$ reductases, Arch. Biochem. Biophys. 474, 283-291.

Aliverti, A., Curti, B, Vanoni, M.A., 1999. Identifying and quantitating FAD and FMN in simple and in iron-sulfur-containing flavoprotein, in: S.K. Chapman, G.A. Reid (Eds.), Flavoprotein Protocols. Vol. 131. Methods in Molecular Biology. Humana Press, Totowa, New Jersey, USA, pp. 9-23.

Baroni, S., Pandini, V., Vanoni, M.A., Aliverti, A., 2012. A single tyrosine hydroxyl group almost entirely controls the NADPH specificity of *Plasmodium falciparum* ferredoxin-NADP$^+$ reductase, Biochemistry 51, 3819-3826.

Batie, C.J., Kamin, H., 1984. Ferredoxin:NADP$^+$ oxidoreductase. Equilibria in binary and ternary complexes with NADP$^+$ and ferredoxin, J. Biol. Chem. 259, 8832-8839.

Bianchi, V., Reichard, P., Eliasson, R., Pontis, E., Krook, M., Jornvall, H., Haggard- Ljungquist, E., 1993. *Escherichia coli* ferredoxin NADP$^+$ reductase: Activation of *E. coli* anaerobic ribonucleotide reduction, cloning of the gene (*fpr*), and overexpression of the protein, J. Bacteriol. 175, 1590-1595.

Ceccarelli, E.A., Arakaki, A.K., Cortez, N., Carrillo, N., 2004. Functional plasticity and catalytic efficiency in plant and bacterial ferredoxin-NADP(H) reductases, Biochim. Biophys. Acta 1698, 155-165.

Correll, C.C., Ludwig, M.L., Bruns, C.M., Karplus, P.A., 1993. Structural prototypes for an extended family of flavoprotein reductases: comparison of phthalate dioxygenase reductase with ferredoxin reductase and ferredoxin, Protein Sci. 2, 2112-2133.

Dym, O., Eisenberg, D., 2001. Sequence-structure analysis of FAD-containing proteins. Protein Sci. 10, 1712-1728.

Ewen, K.M., Kleser, M., Bernhardt, R., 2011. Adrenodoxin: The archetype of vertebrate-type [2Fe-2S] cluster ferredoxins, Biochim. Biophys. Acta 1814, 111-125.

Fukuyama, K., Matsubara, H., Tsukihara, T., Katsube, Y., 1989. Structure of [4Fe-4S] ferredoxin from *Bacillus thermoproteolyticus* refined at 2.3 Å resolution. Structural comparisons of bacterial ferredoxins, J. Mol. Biol. 210, 383-398.

Green, A.J., Munro, A.W., Cheesman, M.R., Reid, G.A., Von Wachenfeldt, C., Chapman, S.K., 2003. Expression, purification and

characterisation of a *Bacillus subtilis* ferredoxin: A potential electron transfer donor to cytochrome P450 BioI, J. Inor. Biochem. 93, 92-99.

Heelis, P.F., 1982. The photophysical and photochemical properties of flavins (isoalloxazines), Chemical Society Reviews 11, 15-39.

Karplus, P.A., Faber, H.R., 2004. Structural aspects of plant ferredoxin: NADP$^+$ oxidoreductases, Photosyn. Res. 81, 303-315.

Knaff, D.B., Hirasawa, M., 1991. Ferredoxin-dependent chloroplast enzymes, Biochim. Biophys. Acta 1056, 93-125.

Komori, H., Seo, D., Sakurai, T., Higuchi, Y., 2010. Crystal structure analysis of *Bacillus subtilis* ferredoxin-NADP$^+$ oxidoreductase and the structural basis for its substrate selectivity, Protein Sci. 19, 2279-2290.

Kurisu, G., Kusunoki, M., Katoh, E., Yamazaki, T., Teshima, K., Onda, Y., Kimata-Ariga, Y., Hase, T., 2001. Structure of the electron transfer complex between ferredoxin and ferredoxin-NADP($^+$) reductase, Nature Struc. Biol. 8, 117-121.

Laemmli, U.K., 1970. Cleavage of structural proteins during the assembly of the head of bacteriophage T4, Nature 227, 680-685.

Lennon, B.W., Williams Jr., C.H., Ludwig, M.L., 2000. Twists in catalysis: alternating conformations of *Escherichia coli* thioredoxin reductase, Science 289, 1190-1194.

Mandai, T., Fujiwara, S., Imaoka, S., 2009a. A novel electron transport system for thermostable CYP175A1 from *Thermus thermophilus* HB27, FEBS J. 276, 2416-2429.

Mandai, T., Fujiwara, S., Imaoka, S., 2009b. Construction and engineering of a thermostable self-sufficient cytochrome P450, Biochem. Biophys. Res. Com. 384, 61-65.

Medina, M., Gómez-Moreno, C., 2004. Interaction of ferredoxin-NADP$^+$ reductase with its substrates: optimal interaction for efficient electron transfer, Photosynth. Res. 79, 113-131.

Moser, C.C., Ross Anderson, J.L., Dutton, P.L., 2010. Guidelines for tunneling in enzymes, Biochim. Biophys. Acta 1797, 1573-1586.

Munro, A.W., Girvan, H.M., McLean, K.J., 2007. Cytochrome P450-redox partner fusion enzymes, Biochim. Biophys. Acta 1770, 345-359.

Muraki, N., Seo, D., Shiba, T., Sakurai, T., Kurisu, G., 2010. Asymmetric dimeric structure of ferredoxin-NAD(P)$^+$ oxidoreductase from the green sulfur bacterium *Chlorobaculum tepidum*: implications for binding ferredoxin and NADP$^+$, J. Mol. Biol. 401,

13

403-414.

Neeli, R., Roitel, O., Scrutton, N.S., Munro, A.W., 2005. Switching pyridine nucleotide specificity in P450 BM3: mechanistic analysis of the W1046H and W1046A enzymes, J. Biol. Chem. 280, 17634-17644.

Nogués, I., Tejero, J., Hurley, J.K., Paladini, D., Frago, S., Tollin, G., Mayhew, S.G., Gómez-Moreno, C., Ceccarelli, E.A., Carrillo, N., Medina, M., 2004. Role of the C-terminal tyrosine of ferredoxin-nicotinamide adenine dinucleotide phosphate reductase in the electron transfer processes with its protein partners ferredoxin and flavodoxin, Biochemistry 43, 6127-6137.

Piubelli, L., Aliverti, A., Arakaki, A.K., Carrillo, N., Ceccarelli, E.A., Karplus, P.A., Zanetti, G., 2000. Competition between C-terminal tyrosine and nicotinamide modulates pyridine nucleotide affinity and specificity in plant ferredoxin-NADP$^+$ reductase. J. Biol. Chem. 275, 10472-10476.

Seo, D., Kamino, K., Inoue, K., Sakurai, H., 2004. Purification and characterization of ferredoxin-NADP$^+$ reductase encoded by *Bacillus subtilis yumC*, Arch. Microbiol. 182, 80-89.

Seo, D., Okabe, S., Yanase, M., Kataoka, K., Sakurai, T., 2009. Studies of interaction of homo-dimeric ferredoxin-NAD(P)$^+$ oxidoreductases of *Bacillus subtilis* and *Rhodopseudomonas palustris*, that are closely related to thioredoxin reductases in amino acid sequence, with ferredoxins and pyridine nucleotide coenzymes, Biochim. Biophys. Acta 1794, 594-601.

Sétif, P., 2001. Ferredoxin and flavodoxin reduction by photosystem I, Biochim. Biophys. Acta 1507, 161-179.

Tejero, J., Perez-Dorado, I., Maya, C., Martinez-Julvez, M., Sanz-Aparicio, J., Gómez-Moreno, C., Hermoso, J.A., Medina, M., 2005. C-terminal tyrosine of ferredoxin-NADP$^+$ reductase in hydride transfer processes with NAD(P)$^+$/H, Biochemistry 44, 13477-13490.

Waksman, G., Krishna, T.S., Williams Jr., C.H., Kuriyan, J., 1994. Crystal structure of *Escherichia coli* thioredoxin reductase refined at 2 Å resolution. Implications for a large conformational change during catalysis, J. Mol. Biol. 236, 800-816.

Yagi, K., Ohishi, N., Nishimoto, K., Choi, J.D., Song, P.S., 1980. Effect of hydrogen bonding on electronic spectra and reactivity of flavins, Biochemistry 19, 1553-1557.

Figure legends

Fig. 1 (A) Close-up view of the C-terminal extension in the crystal structure of *Bs*FNR (PDB code: 3LZX). The figure was prepared using Discovery Studio 3.5 Visualizer (Accelrys Inc., USA). Side chains of Tyr313 and His324 are depicted as ball and stick model. Subunits A and B and helix 6 are colored in blue, green and purple, respectively. (B) Partially aligned amino acid sequences of the C-terminal region of TrxR-type FNRs. The numbers of amino acid residues in *Bs*FNR are indicated. The His324 residue of *Bs*FNR is indicated by an arrow. The positions of the 6th and 7th helices assigned in the crystal structure of *Bs*FNR (Komori et al., 2010) are indicated by rods. BSU_32110: FNR from *Bacillus subtilis* subsp. *subtilis str. 168* (this work), rpa_RPA3954: *Rhodopseudomonas palustris* CGA009 FNR, tth_TTC0096: *Thermus thermophilus* HB27 FNR, cte_CT1512: *Chlorobaculum tepidum* FNR.

Fig. 2 (A) UV-visible absorption spectra of WT and mutated *Bs*FNRs in the air-oxidized form. Measurements were performed at room temperature in 20 mM HEPES-NaOH buffer (pH 7.0). Solid line: WT *Bs*FNR, dotted line: ΔY313, broken line: ΔS325. (B) Difference spectra induced by an addition of 1 mM NADP$^+$. Solid line: WT *Bs*FNR, dotted line: ΔY313, broken line: ΔS325. Measurements were performed at room temperature in 20 mM HEPES-NaOH buffer (pH 7.0). (C) Relationship between the magnitude of spectral change and NADP$^+$ concentration. WT *Bs*FNR ($\bullet$): $\Delta\varepsilon_{505}$ - $\Delta\varepsilon_{481}$, ΔY313 *Bs*FNR ($\circ$): $\Delta\varepsilon_{506}$ - $\Delta\varepsilon_{481}$, and ΔS325 *Bs*FNR ($\square$): $\Delta\varepsilon_{506}$ - $\Delta\varepsilon_{480}$. Each 1–10 μl of NADP$^+$ (0.01 – 100 mM) stock solutions were added to the cuvettes containing 2 ml of ~ 10 μM *Bs*FNR solutions in 20 mM HEPES-NaOH buffer (pH 7.0) for the sample cell and 20 mM HEPES-NaOH buffer (pH 7.0) only for the reference cell.

Fig. 3 Effect of Fd concentration on the cytochrome *c* reduction activity of WT and ΔS325 *Bs*FNRs. Assays were performed in 20 mM HEPES-NaOH buffer (pH 7.0) at 25 °C. Reaction mixtures contained 5 mM G6P, 5 U ml^{-1} G6PDH, 0.1 mM horse heart cytochrome *c*, 5 μM NADPH and 5 nM *Bs*FNRs with *B. subtilis* Fd as indicated. Observed rates are expressed by subtraction of the respective assay blank containing all the assay reagents except FNRs. Error bar at each data point represents ± one standard deviations.

Table 1

Enzymatic, spectroscopic and molecular properties of WT and mutant BsFNRs

	WT	$\mathit{\Delta}$Y313	$\mathit{\Delta}$S325
NADPH diaphorase with ferricyanide*			
K_m for NADPH (μM)[a]	20 ± 1	10.7 ± 0.4	8.7 ± 0.4
K_m for ferricyanide (μM)[b]	290 ± 20	990 ± 90	1600 ± 160
k_{cat} (s[-1])[a]	930 ± 11	872 ± 7	1050 ± 10
K_d for NADP^{+} (μM)[c]*	4.6 ± 0.2	1.5 ± 0.2	1.5 ± 0.2
ε (mM[-1]cm^{-1} per subunit) / at λ max (nm)	12.3/ 457[d]	12.6/ 457	12.3/ 457
App. M_r (gel-permeation/ SDS-PAGE, kDa)	97 / 40	94 / 38	94 / 40

*Each parameter value is represented ± one standard deviation.

a: at 4 mM ferricyanide

b: at 1 mM NADPH

c: obtained with the data in Figure 2C
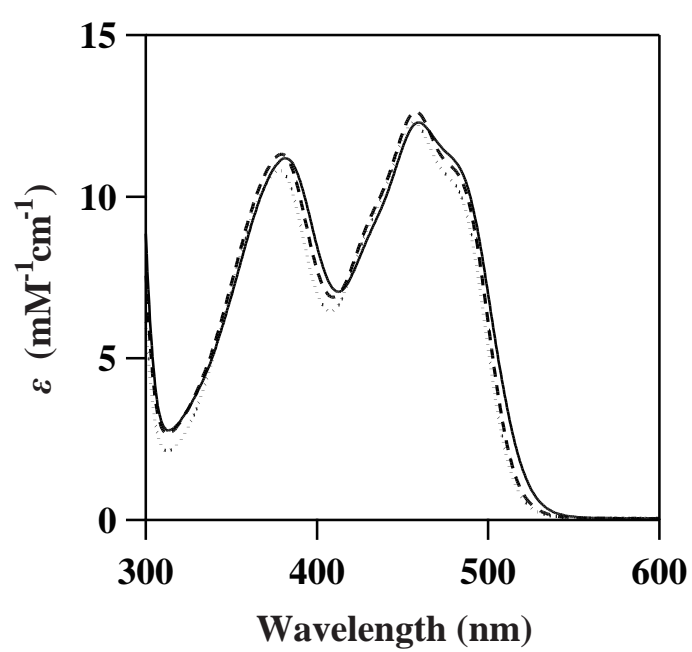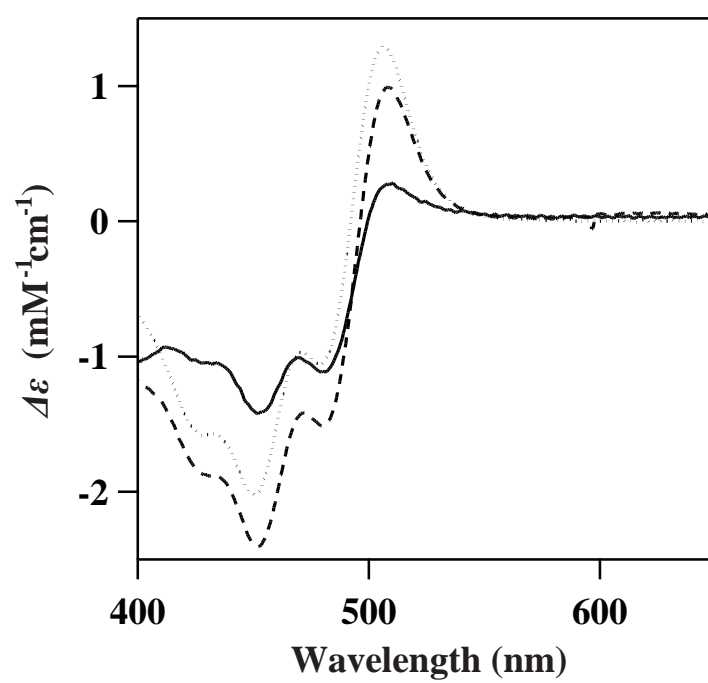
d: from (Seo et al., 2004)

Figure 1A

Figure 1B

```
                         300              α6                  320       ↓    α7
                          •       ▬▬▬▬▬▬▬▬▬▬▬▬▬▬              •              ▬▬▬
bsu_BSU32110    ...FGEAPTAVNNAKAYMDPKARVQPLHSTSLFENK----------------
rpa_RPA3954     ...FHEGALMAQKAVKYVYPDKRVVFQYTTSSTNLQKKLGVN---------
tth_TTC0096     ...FGEAAIAANHAAAYANPALKVNPGHSSEKAAPGT-------------
cte_CT1512      ...LSEATMAVRHSLSYIKPGEKIRNVFSSVKMAKEKKAAEAGNATENKAE
                    :  *..    ..::     *    *   ::     .::
```
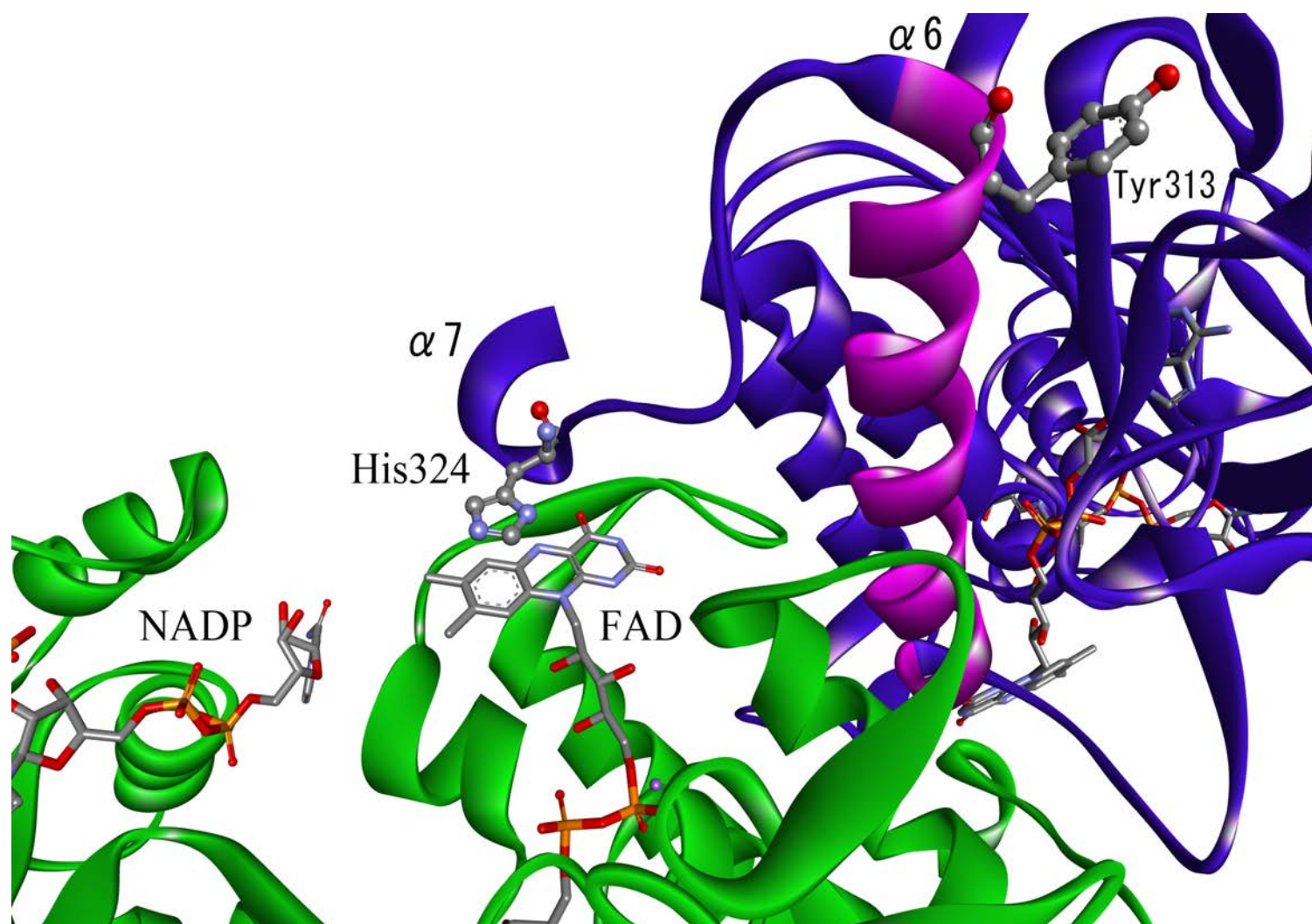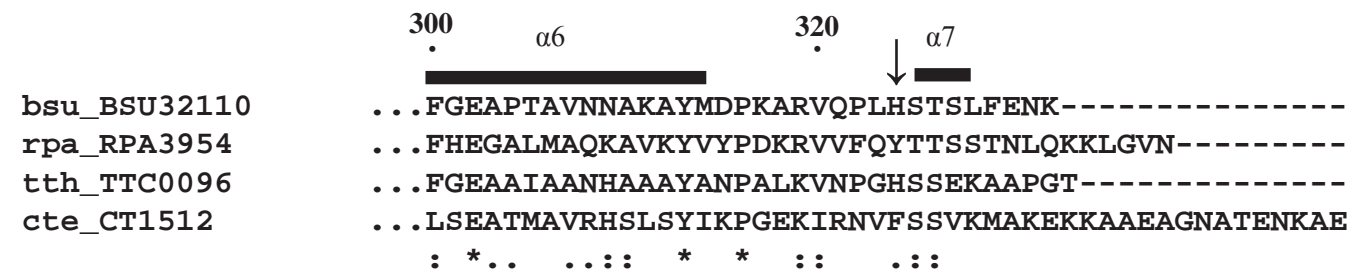
Figure 2A

Figure 2B

Figure 2C
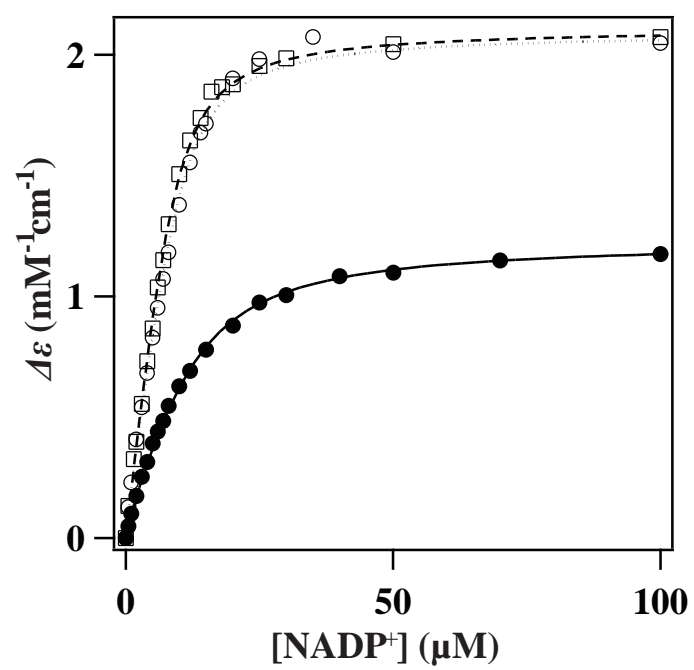
Figure 3
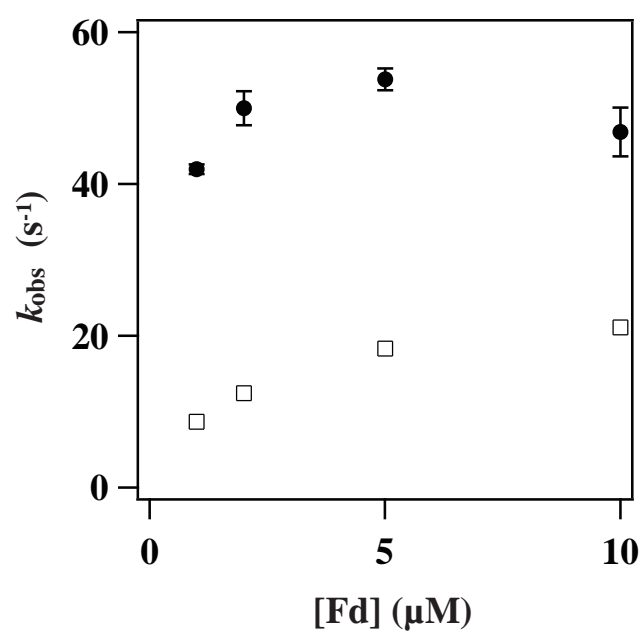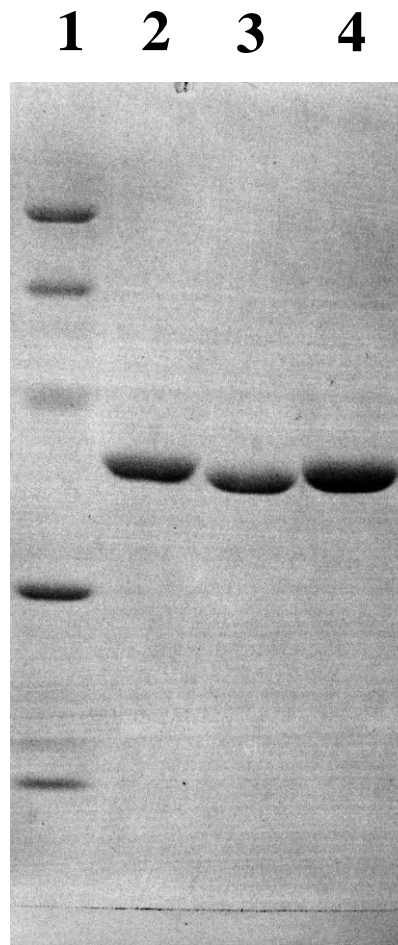
Figure S1
SDS-PAGE analysis of wild type and mutated *Bs*FNR proteins with Coomassie Brilliant Blue staining. Lanes 1–4 were loaded with molecular weight markers (97.4, 66.2, 45.0, 32.0, 21.0, 14.4 kDa from the top), wild type, *Δ*Y313 and *Δ*S325 mutants, respectively.
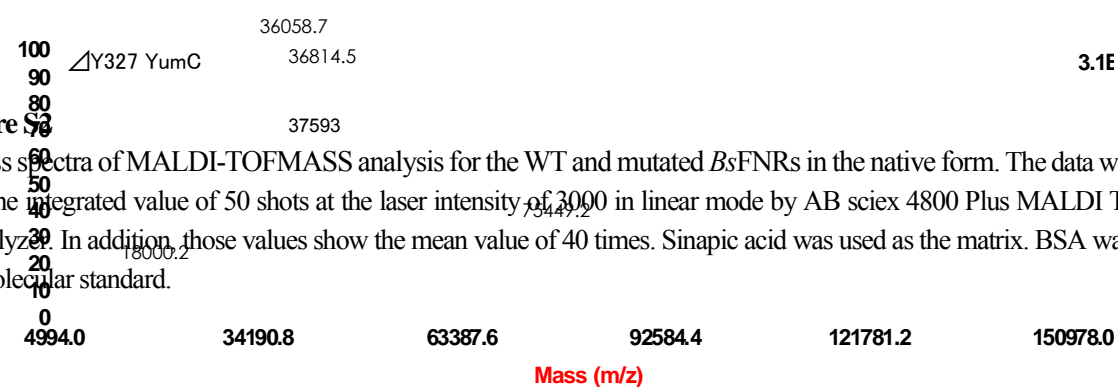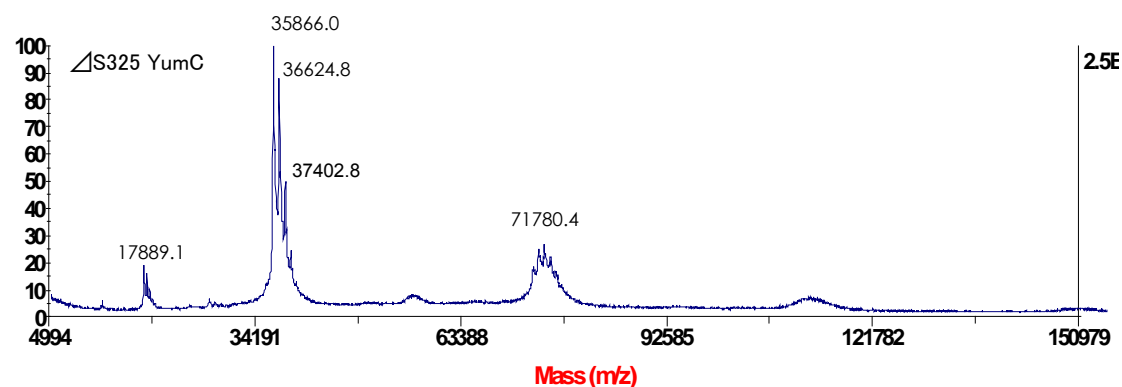
WT YumC

2.5E

36749.4
37523.7
38294.8
18341.4
74308.9

Mass (m/z)

△Y313 YumC

3.6E

34431.3
35179.6
35971
17180.2
68908.5

Mass (m/z)

△S325 YumC

2.5E

35866.0
36624.8
37402.8
17889.1
71780.4

Mass (m/z)

△Y327 YumC

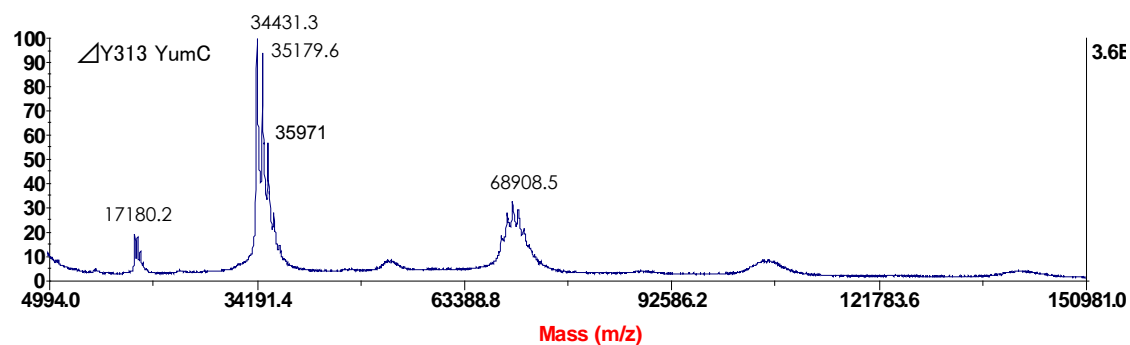3.1E

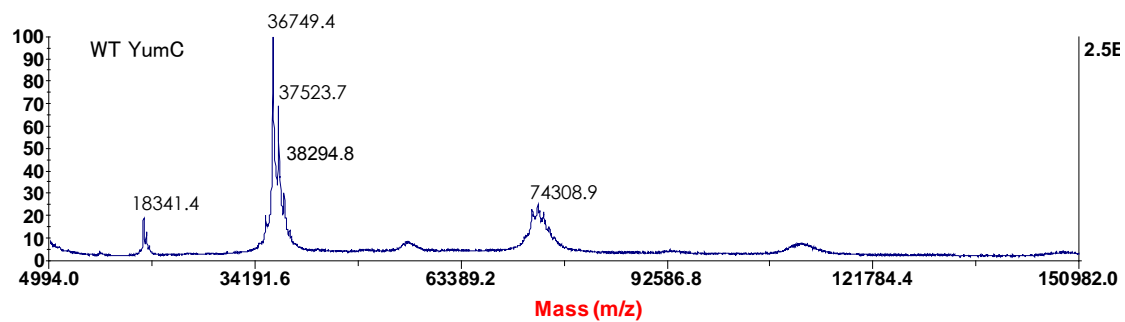36058.7
36814.5
37593
18000.2
75447.2

Mass (m/z)

Figure S3

Mass spectra of MALDI-TOFMASS analysis for the WT and mutated *Bs*FNRs in the native form. The data were obtained by the integrated value of 50 shots at the laser intensity of 3000 in linear mode by AB sciex 4800 Plus MALDI TOF/TOF™ Analyzer. In addition, those values show the mean value of 40 times. Sinapic acid was used as the matrix. BSA was utilized as a molecular standard.
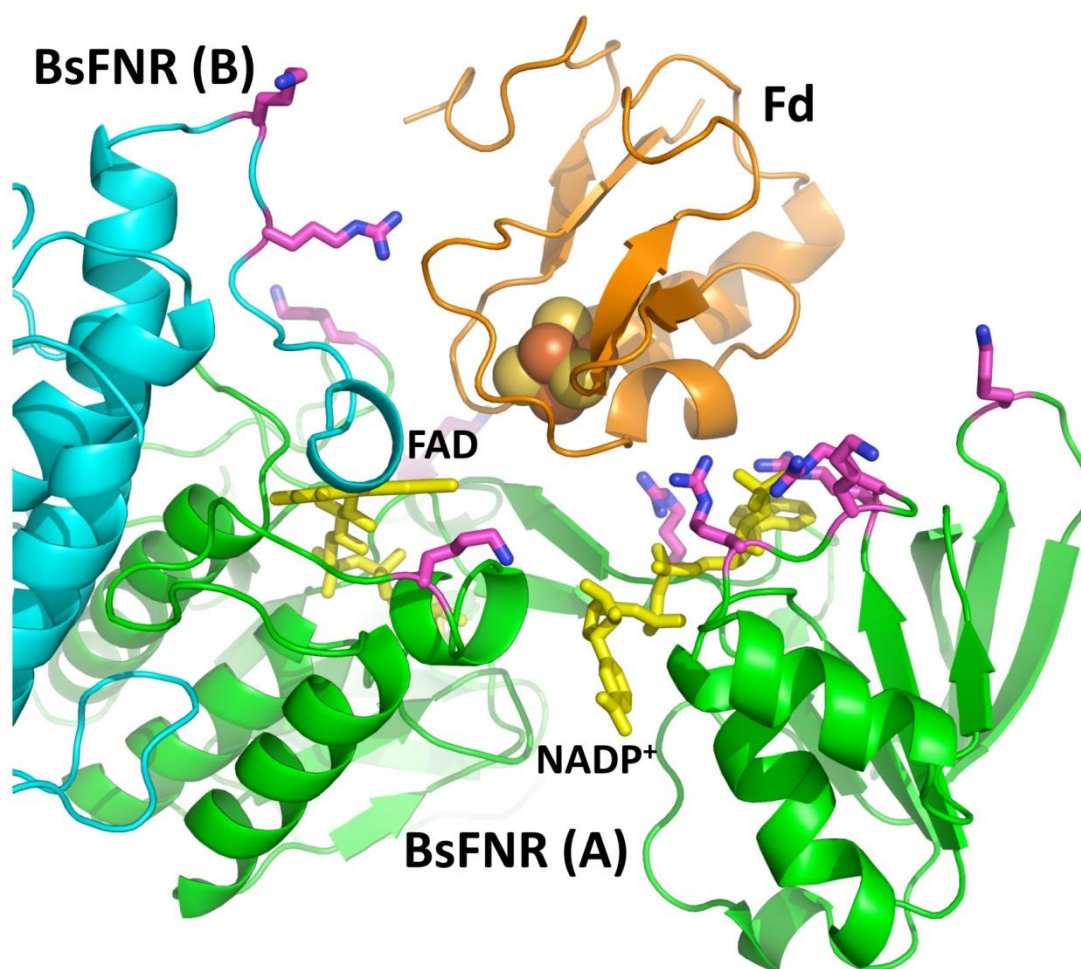
Figure S3

Docking model of *Bacillus thermoproteolyticus* Fd (*Bt*Fd) and *Bacillus subtilis* FNR (*Bs*FNR). *Bt*Fd (PDB ID: 1IQZ) was docked to a large cleft between two domains of *Bs*FNR (PDB ID: 3LZX) without any steric hindrance using the programs COOT (Emsley, P. & Cowtan, K., Acta Crystallogr D Biol. Crystallogr. (2004) 60, 2126-2132). In the model, both proteins are considered as the rigid bodies. The distance between the Fe2 atom of the [4Fe-4S] cluster on *Bt*Fd and the C8M atom of the FAD on *Bs*FNR is 8.8 Å. The figures were prepared with PyMOL (http://pymol.sourceforge.net). *Bs*FNR molecules A and B are shown in green and cyan, respectively. FAD and NADP$^+$ molecules are shown in yellow. *Bt*Fd is shown in orange. Positively charged residues around the large cleft between the two domains of *Bs*FNR are shown in magenta.

Table S1

Nucleotide sequences of the forward (-F) and reverse (-R) primers utilized for the preparation of mutated *Bs*FNR genes. The positions of the produced termination codons in the sequence are underlined.

Primer name	Nucleotide sequence
yumC-Y313del-F	GAA CAA CGC CAA GGC T**TA A**AT GGA CCC GAA AGC CCG
yumC-Y313del-R	CGG GCT TTC GGG TCC AT**T TA**A GCC TTG GCG TTG TTC
yumC-S325del-F	GCC CGC GTA CAG CCT CTT CAC **TAA** ACA AGT CTT TTT G
yumC-S325del-R	CAA AAA GAC TTG T**TT A**GT GAA GAG GCT GTA CGC GGG C